Aalto University

OPEN ACCESS

This is an electronic reprint of the original article.
This reprint may differ from the original in pagination and typographic detail.

Liu, Hanchen; Pasanen, Toni; Fung, John; Isometsä, Joonas; Leiviskä, Oskari; Vähänissi, Ville; Savin, Hele

Comparison of SiNx-based Surface Passivation Between Germanium and Silicon

Published in:
Physica Status Solidi (A) Applications and Materials Science

DOI:
10.1002/pssa.202200690

Published: 01/01/2023

Document Version
Publisher's PDF, also known as Version of record

Published under the following license:
CC BY

Please cite the original version:
Liu, H., Pasanen, T., Fung, J., Isometsä, J., Leiviskä, O., Vähänissi, V., & Savin, H. (2023). Comparison of SiNx-based Surface Passivation Between Germanium and Silicon. *Physica Status Solidi (A) Applications and Materials Science*, *220*(2), Article 2200690. https://doi.org/10.1002/pssa.202200690

This material is protected by copyright and other intellectual property rights, and duplication or sale of all or part of any of the repository collections is not permitted, except that material may be duplicated by you for your research use or educational purposes in electronic or print form. You must obtain permission for any other use. Electronic or print copies may not be offered, whether for sale or otherwise to anyone who is not an authorised user.

physica status solidi a
www.pss-a.com

Check for updates

Comparison of SiN_x-Based Surface Passivation Between Germanium and Silicon

*Hanchen Liu, Toni P. Pasanen, Tsun Hang Fung, Joonas Isometsä, Oskari Leiviskä, Ville Vähänissi, and Hele Savin**

Germanium (Ge) has attracted much attention as a promising channel material in nanoscale metal–oxide–semiconductor devices and near-infrared sensing because of its high carrier mobilities and narrow bandgap, respectively. However, efficient passivation of Ge surfaces has remained challenging. Herein, silicon nitride (SiN_x)-based passivation schemes on Ge surfaces are studied and the observations are compared to Si counterparts. These results show that instead of a high positive charge density (Q_{tot}) that is found in SiN_x-passivated Si samples, similar Ge samples contain a high amount of negative Q_{tot} (in the range of 10^{12} cm^{-2}). The maximum surface recombination velocity of the samples is shown to reduce by a factor of three in both Si and Ge samples by a post-deposition anneal at 400 °C. The SiN_x-coated samples are capped with an atomic-layer-deposited aluminum oxide (Al_2O_3) layer, which reduces the midgap interface defect density (D_{it}) after annealing to 7×10^{10} and 4×10^{11} cm^{-2} eV^{-1} in Si and Ge, respectively. Interestingly, while the Al_2O_3 capping seems to have no impact on Q_{tot} of the Si samples, it turns the stack virtually neutral ($\sim -1.6 \times 10^{11}$ cm^{-2}) on Ge. The presented SiN_x-based passivation schemes are promising for optoelectronic devices, where a low D_{it} and/or a low charge are favored.

1. Introduction

Germanium (Ge) draws currently attention as an attractive material for many applications. The high intrinsic carrier mobility makes it a potential candidate to replace silicon (Si) as an active channel material in future high-performance metal–oxide–semiconductor (MOS) devices.[1] The narrow bandgap ($\sim$0.66 eV) makes it also an attractive material for photovoltaic devices and sensors, such as the bottom cell of multijunction solar cells and near-infrared (NIR) photodetectors.

H. Liu, T. P. Pasanen, T. H. Fung, J. Isometsä, O. Leiviskä, V. Vähänissi, H. Savin
Department of Electronics and Nanoengineering
Aalto University
Tietotie 3, FI-02150 Espoo, Finland
E-mail: hele.savin@aalto.fi

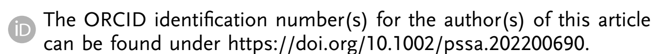
The ORCID identification number(s) for the author(s) of this article can be found under https://doi.org/10.1002/pssa.202200690.

© 2022 The Authors. physica status solidi (a) applications and materials science published by Wiley-VCH GmbH. This is an open access article under the terms of the Creative Commons Attribution License, which permits use, distribution and reproduction in any medium, provided the original work is properly cited.

DOI: 10.1002/pssa.202200690

In all these devices, the reduction of charge carrier recombination at Ge surfaces and interfaces is crucial. However, the passivation of Ge surfaces has historically been challenging due to the lack of a stable oxide. For instance, the high amount of interface traps, especially the acceptor-like trap states, has been a concern in Ge-based NMOS field-effect transistors due to the resulting mobility degradation.[2]

The density of interface defect states (D_{it}) has earlier been successfully reduced by generating a high-quality germanium dioxide (GeO_2) layer at the surface. Yukio et al. obtained a high-quality Ge/GeO_2 interface by using a low-temperature electron cyclotron resonance (ECR)-generated oxygen plasma stream and achieved a midgap D_{it} of $\sim 4.5 \times 10^{10}$ cm^{-2} eV^{-1} with an atomic-layer-deposited (ALD) aluminum oxide (Al_2O_3) capping.[3] Bellenger et al. achieved a D_{it} of $\sim 2 \times 10^{11}$ cm^{-2} eV^{-1} at the midgap by thermally growing GeO_2 in molecular oxygen, followed by the deposition of an ALD Al_2O_3 or hafnium oxide (HfO_2) capping.[4] Kuzum et al. realized a Ge/GeO_2 interface by using ozone oxidation at 400 °C and achieved a minimum D_{it} of 3×10^{11} cm^{-2} eV^{-1}.[5]

Besides reducing the interface defects, surface passivation can be improved via field-effect passivation. Some progress on this topic has recently been achieved: Isometsä et al. achieved a low surface recombination velocity (SRV) of 6.55 cm s^{-1} and a high negative charge density (Q_{tot}) over -2×10^{12} cm^{-2} by ALD Al_2O_3 combined with a hydrochloric acid (HCl) pre-treatment.[6] Simultaneously, Berghuis et al. reported an exceptionally high negative Q_{tot} of $\sim -1 \times 10^{13}$ cm^{-2} and a low SRV of $\sim$2.6 cm s^{-1} using a hydrogenated amorphous silicon (a-Si:H)/Al_2O_3 stack, synthesized by plasma-enhanced chemical vapor deposition (PECVD) and plasma-enhanced ALD (PEALD), respectively.[7]

The aforementioned research on field effect passivation of Ge has focused on ALD Al_2O_3 which is known to have a high negative charge. Another promising material that utilizes strong field-effect passivation is silicon nitride (SiN_x) deposited by PECVD. This material is commonly used for example in Si solar cells as it provides efficient surface passivation thanks to its high positive Q_{tot}.[8] The hydrogenated SiN_x provides also excellent chemical passivation, which is activated by post-deposition anneal (PDA).[9] Some preliminary results on the passivation of Ge

© 2022 The Authors. physica status solidi (a) applications and materials science published by Wiley-VCH GmbH

18626319, 2023, 2, Downloaded from https://onlinelibrary.wiley.com/doi/10.1002/pssa.202200690 by Aalto University, Wiley Online Library on [05/02/2023]. See the Terms and Conditions (https://onlinelibrary.wiley.com/terms-and-conditions) on Wiley Online Library for rules of use; OA articles are governed by the applicable Creative Commons License

18626319, 2023, 2, Downloaded from https://onlinelibrary.wiley.com/doi/10.1002/pssa.202200690 by Aalto University, Wiley Online Library on [05/02/2023]. See the Terms and Conditions (https://onlinelibrary.wiley.com/terms-and-conditions) on Wiley Online Library for rules of use; OA articles are governed by the applicable Creative Commons License

via PECVD SiN_x have also been reported, but the data available is still rather limited.[10,11]

It is rather common to enhance the passivation of Si surfaces by capping the PECVD films with another thin film, such as Al_2O_3. During a subsequent anneal, the Al_2O_3 capping layer acts both as a hydrogen source as well as a hydrogen diffusion barrier, which enables efficient hydrogen diffusion to the Si–thin-film interface and consequently a high level of chemical passivation.[12–14] This approach has been used for several different thin films on Si, including PECVD SiO_2 and SiN_x.[14,15] However, research on a similar approach for the passivation of Ge is limited.

In this work, we study SiN_x-based passivation schemes on Ge surfaces and compare our observations to Si counterparts. We study the passivation performance both without and with post-deposition annealing. We also investigate the impact of an Al_2O_3 capping layer on the passivation efficiency. To get more understanding of the Ge–thin-film interface properties, we complement our studies with corona charging experiments.

2. Experimental Section

Figure 1 outlines the process flow of the experiments. The same process was applied to both Ge and Si wafers. The Ge substrates were 175 μm thick n-type (antimony-doped) Czochralski-grown (CZ) wafers with <100> orientation, 50 mm diameter, and 5–15 Ωcm resistivity. The Si substrates were 280 μm thick n-type (phosphorous-doped) Float-zone (FZ) wafers with <100> orientation, 100 mm diameter, and 1–5 Ωcm resistivity. To clean the wafers and to remove the native oxide, the Ge wafers were dipped to 31.6% HCl for 90 s without a (consecutive) de-ionized water (DIW) rinse,[6] whereas the Si wafers were cleaned by the standard RCA cleaning sequence with a hydrofluoric acid (HF) dip for 90 s followed by DIW rinsing as the last step. After the cleaning, a 20 nm-thick SiN_x layer was deposited on both sides of the Ge and Si substrates using a radio-frequency (RF, 13.56 MHz) PECVD system (Plasmalab 80 Plus) at 380 °C with silane (SiH_4, gas flow 17.5 sccm), ammonia (NH_3, gas flow 50 sccm) and nitrogen (N_2, gas flow 332.5 sccm) as the precursor gases. The pressure was 1000 mTorr, and the plasma power was 25 W. An additional double-sided 20 nm-thick Al_2O_3 capping layer was deposited on some of the samples to create a SiN_x/Al_2O_3 stack. The deposition was done by thermal ALD at 200 °C using trimethylaluminum (TMA) and H_2O precursors. To study the impact of heat treatment on surface passivation, the samples were annealed at 400 °C in an ATV PEO-601 furnace for 30 min in forming a gas (FG, 95% N_2 + 5% H_2) atmosphere. The anneal temperature was limited to 400 °C, which is somewhat lower than the typical temperature used for SiN_x in silicon solar cells. This is because dopants diffuse faster in Ge than in Si,[16,17] and hence much higher temperatures cannot be applied to Ge-based devices without affecting doped p-n junctions or other diffused regions. The lower temperature also helps to avoid severe blistering that is often encountered in annealed SiN_x films.[18]

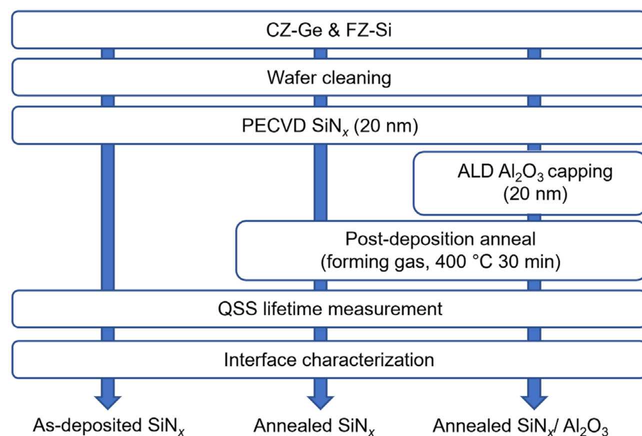

Figure 1. Process flow for the studied samples showing the most important processing and characterizing steps.

To study the effectiveness of surface passivation obtained via the applied thin films, injection-level-dependent effective minority carrier recombination lifetime (τ_{eff}) was measured by quasi-steady-state microwave photoconductance decay (QSS-μPCD) with Semilab PV2000A. The τ_{eff} was additionally measured from some of the Si samples using the transient photoconductance technique with Sinton Instruments WCT-120TS. To more directly evaluate the amount of surface recombination, infinite bulk lifetime was assumed and the resulting maximum surface recombination velocity (SRV_{max}) was calculated by the equation

$$SRV_{max} = \frac{W}{2*\tau_{eff}} \tag{1}$$

where W is the wafer thickness. The SRV_{max} is reported around the excess minority carrier density (Δn) that yielded the highest lifetime within the measured injection level range, i.e., 1×10^{14} and 1×10^{15} cm^{-3} for Ge and Si, respectively.

A corona charge (Q_c) lifetime experiment was performed to obtain information on the polarity and magnitude of Q_{tot}.[7,19,20] For this measurement, the samples were cleaved into halves. For one of the halves, negative Q_c was uniformly deposited on both sides in a gradual manner by a linear corona charger to modulate the field-effect passivation. The exact amount of the deposited Q_c was determined by measuring the potential change over the sample using a Kelvin probe-based measurement setup. After each incremental charging step, the SRV_{max} was calculated from the measured carrier lifetime. The measurement was repeated for the other half of the sample, in the same manner, using positive Q_c. Finally, the Q_{tot} and D_{it} were assessed with the corona oxide characterization of semiconductor (COCOS) method by Semilab PV2000A from the samples with a SiN_x/Al_2O_3 stack to obtain more quantitative information on the interface properties.

3. Results

Figure 2a shows the injection-level-dependent minority carrier lifetime of the Si and Ge samples passivated by 20 nm of SiN_x. On the Si substrate, the as-deposited SiN_x provides only limited surface passivation with a maximum lifetime of 100 μs (minority carrier diffusion length L_p = 346 μm, SRV_{max} = 140 cm s^{-1}). Surface passivation is enhanced after a PDA by a factor of three, and a τ_{eff} of ~300 μs is achieved (L_p = 600 μm, SRV_{max} = 46 cm s^{-1}). The obtained results are

© 2022 The Authors. physica status solidi (a) applications and materials science published by Wiley-VCH GmbH

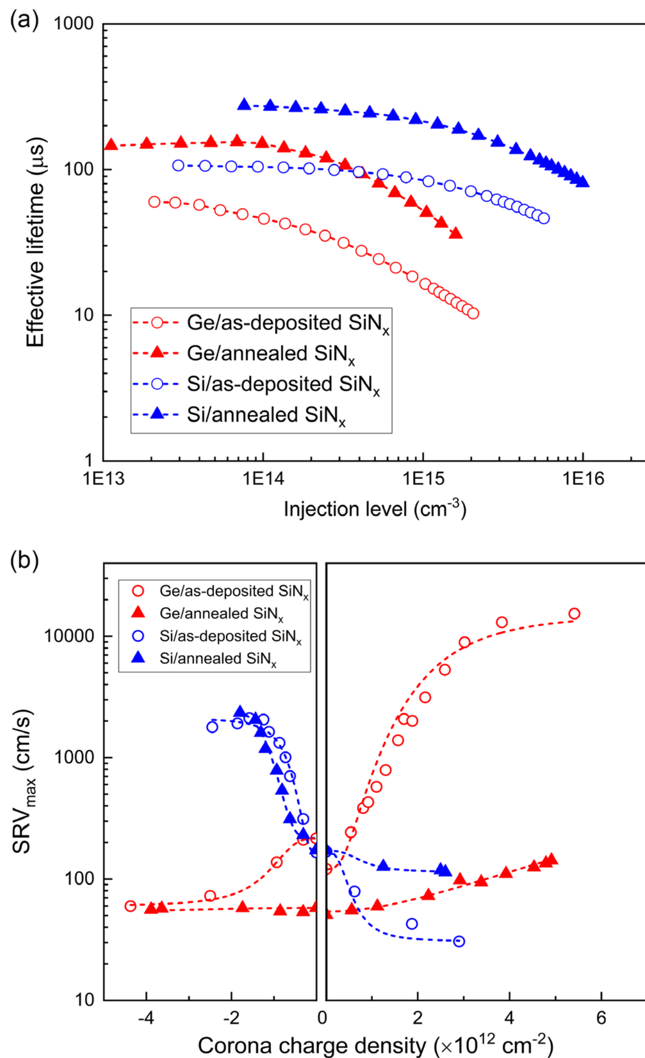

Figure 2. a) Injection-level-dependent effective minority carrier lifetime and b) surface recombination velocity versus deposited corona charge density for Ge and Si samples passivated by SiN_x in the as-deposited and annealed state. The dashed lines are guides for the eyes.

consistent with the literature, which shows that a similar improvement can be achieved with a 400 °C PDA.[21] A higher temperature would likely result in a larger improvement,[21] however, it is not practical for Ge-based devices as discussed earlier. Similar behavior is observed on the Ge substrate but with a slightly higher SRV_{max}: the as-deposited SiN_x passivated sample has a maximum lifetime of ~60 µs ($L_p = 542$ µm, $SRV_{max} = 146$ cm s^{-1}) and after a PDA the τ_{eff} increases to 150 µs ($L_p = 857$ µm, $SRV_{max} = 58$ cm s^{-1}).

To study the polarity of Q_{tot}, SRV_{max} was measured as a function of Q_c. The effect of added Q_c on SRV_{max} is shown in Figure 2b. The SRV_{max} of the as-deposited Si/SiN_x sample increases with added negative Q_c, while it reduces with added positive Q_c. This indicates that the SiN_x film on Si has a positive Q_{tot} (the order of magnitude is ~10^{12} cm^{-2}). The surface is thus initially in accumulation, which transforms towards depletion when adding negative Q_c resulting in weaker field effect passivation (SRV_{max} increases). The high positive Q_{tot} is a well-known property of SiN_x on Si and hence the result is consistent with previous studies.[22,23] Interestingly, the Ge samples passivated with as-deposited SiN_x show an opposite trend: the SRV_{max} reduces with added negative Q_c, while it increases with added positive Q_c. This indicates the presence of a negative Q_{tot} (in the range of 10^{12} cm^{-2}) within the thin film. A similar observation (i.e., a negative Q_{tot} within SiN_x film on the Ge surface) has been reported recently by Berghuis et al.[10]

The PDA seems to have almost no impact on the trend of SRV_{max} of Si/SiN_x samples as a function of Q_c: both the polarity and magnitude of Q_{tot} remain similar which is in agreement with previous studies.[24] In contrast, for the Ge/SiN_x samples, the charge polarity remains the same but the SRV_{max} behaves differently as a function of Q_c after the PDA, indicating changes in the magnitude of Q_{tot}.

To study the effect of a capping layer on surface passivation, a 20 nm thick ALD Al_2O_3 thin film was deposited on top of the SiN_x layer. The bar plot in **Figure 3**a presents the τ_{eff} of Ge and Si passivated with as-deposited SiN_x, annealed SiN_x, and annealed SiN_x/Al_2O_3 stack. The results demonstrate that the Al_2O_3 capping has a much larger impact on the surface passivation than a PDA alone for both substrates. For Si, the enhancement is very impressive with a τ_{eff} of around 7 ms ($L_p = 2898$ µm, $SRV_{max} = 2$ cm s^{-1}) in the SiN_x/Al_2O_3-passivated sample, which agrees with earlier reports on similar improvements with Al_2O_3 capping.[13,25] For Ge, the annealed SiN_x/Al_2O_3 stack results in a lifetime of around 500 µs ($L_p = 1565$ µm, $SRV_{max} = 17.5$ cm s^{-1}), which is more than double as compared to the bare SiN_x film, although the enhancement is much smaller than in Si counterpart. It is good to note that here the Ge bulk likely has an impact on the measured lifetime, since we achieved only a slightly higher lifetime of ~800 µs from the same substrate material using well-optimized Al_2O_3 surface passivation.[6] This means that the SRV for the Ge sample with the annealed SiN_x/Al_2O_3 stack is in reality somewhat lower than the calculated maximum value.

To get more understanding of the interface properties of the samples passivated with the SiN_x/Al_2O_3 stack, the Q_{tot} and D_{it} were quantitatively characterized by the COCOS method, as shown in Figure 3b,c. In Si, the measured Q_{tot} is $+2.7 \times 10^{12}$ cm^{-2} indicating that the Al_2O_3 capping has no influence on the field effect passivation. Interestingly, the charge density of the Ge samples has reduced drastically, and the thin film stack is virtually neutral (~-1.6×10^{11} cm^{-2}). This means that the capping layer affects the field-effect passivation of Ge surfaces rather dramatically.

Figure 3c presents the D_{it} distribution within the bandgap for the same samples. The midgap D_{it} of the Si samples passivated with the stack is ~7×10^{10} cm^{-2} eV^{-1}, which demonstrates an excellent level of chemical passivation.[12–15] Indeed, the low amount of interface defects combined with the high Q_{tot} explains the very high τ_{eff} reported in Figure 3a. In the case of Ge, the midgap D_{it} is ~4×10^{11} cm^{-2} eV^{-1}, which is low enough for enabling highly-efficient optoelectronic devices, such as solar cells and photodetectors.[26,27] Interestingly, the midgap D_{it} achieved with the SiN_x/Al_2O_3 stack on Ge is lower than recently reported for PEALD Al_2O_3-passivated Ge (~1×10^{12} cm^{-2} eV^{-1}).[7] The improvement in surface passivation obtained with the capping layer is indeed mainly due to

© 2022 The Authors. physica status solidi (a) applications and materials science published by Wiley-VCH GmbH

18626319, 2023, 2, Downloaded from https://onlinelibrary.wiley.com/doi/10.1002/pssa.202200690 by Aalto University, Wiley Online Library on [05/02/2023]. See the Terms and Conditions (https://onlinelibrary.wiley.com/terms-and-conditions) on Wiley Online Library for rules of use; OA articles are governed by the applicable Creative Commons License

18626319, 2023, 2, Downloaded from https://onlinelibrary.wiley.com/doi/10.1002/pssa.202200690 by Aalto University, Wiley Online Library on [05/02/2023]. See the Terms and Conditions (https://onlinelibrary.wiley.com/terms-and-conditions) on Wiley Online Library for rules of use; OA articles are governed by the applicable Creative Commons License

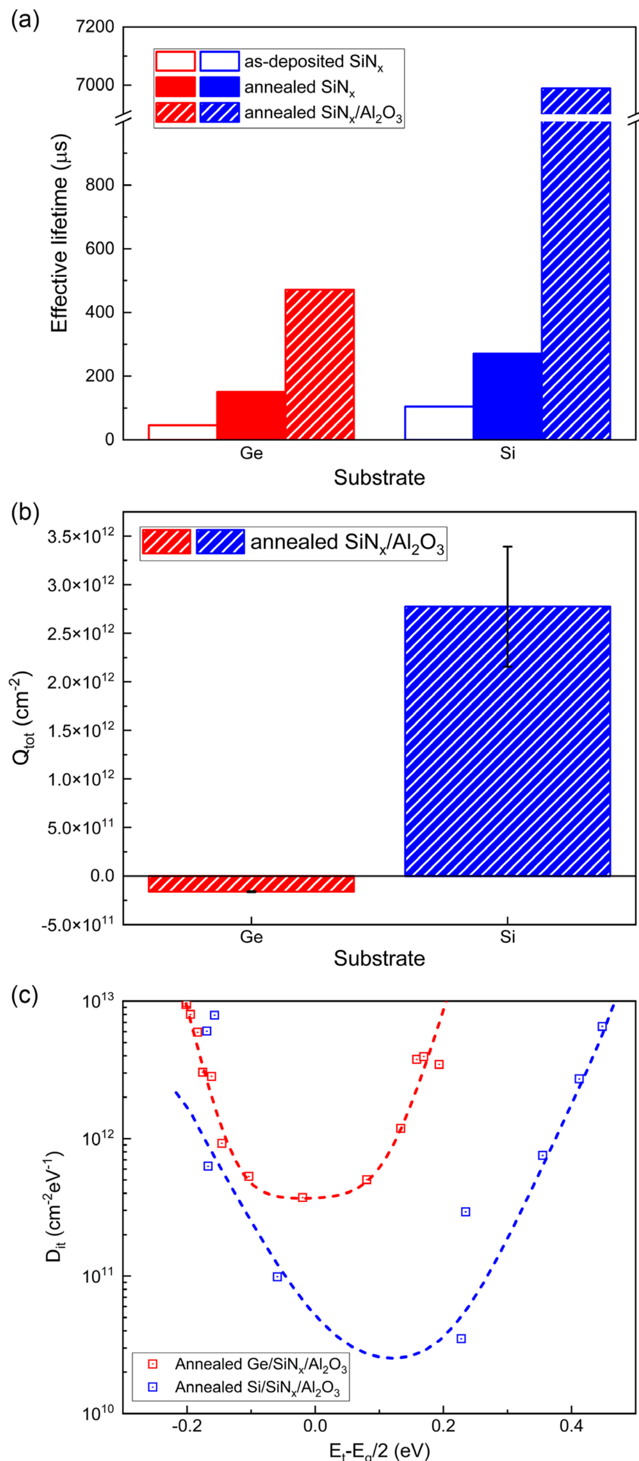

Figure 3. a) The minority carrier lifetime of Ge and Si samples passivated by as-deposited SiN_x, annealed SiN_x, and annealed SiN_x/Al_2O_3 stack at the injection level of 1×10^{14} cm^{-3}. b) Q_{tot} and c) D_{it} for Ge and Si samples passivated with annealed SiN_x/Al_2O_3 measured by corona oxide characterization of semiconductor (COCOS). The dashed lines are guides to the eyes.

the excellent chemical passivation, since the Q_{tot} of the samples is virtually zero, providing only weak field-effect passivation. Hence, the SiN_x/Al_2O_3 stack would be optimal for Ge surface passivation in applications where field-effect cannot be utilized.

4. Discussion

SiN_x on Si usually exhibits a high positive Q_{tot} (typically several times 10^{12} cm^{-2}), which is very beneficial e.g., for n-type emitters on solar cells with a p-type substrate.[28,29] This high density of charge originates from the predominant defects, the threefold coordinated Si atoms (·Si≡N3), called K centers.[30] They contribute positive charges when turning into stable states +Si≡N3 (K+ centers) on Si substrate.[29] Unexpectedly, it was found earlier that SiN_x on Ge contains a negative charge instead of a positive charge. One possible explanation for this overall negative Q_{tot} could be the Ge surface trap states and the amphoteric property of the K centers. The position of the charge neutrality level (CNL) at the Ge surface is determined by the weights of acceptor-like and donor-like states. If the Fermi level is higher than the CNL, the ionized acceptor-like states will lead to a negative charge at the interface. In contrast, if the Fermi level is lower than the CNL, the empty donor-like states will build a positive interface charge. Since there is a large number of acceptor-like states, which consist of dangling bonds (DBs), the bond strain, vacancies, and Ge ad-atom formation,[31–33] the position of the CNL in Ge is located very close to the valence band, only ~0.09 eV above it.[34,35] In addition, the Fermi level at the interface overlaps the CNL, regardless of the doping type of Ge, causing Fermi level pinning.[34] These unpassivated interface trap states could contribute to the measured high negative Q_{tot}. Moreover, the amphoteric K centers of SiN_x can also be occupied by a negative charge with the following reactions

$$K^0 + e^- \rightarrow K^- \quad (2)$$

$$K^+ + 2e^- \rightarrow K^- \quad (3)$$

We speculate that those K^- centers originate from the electron injection from the high density of ionized acceptor-like states and the band alignment. This indicates that the polarity of Q_{tot} on Ge interface heavily relies on the passivation of the surface trap states.

The well-known hydrogenation passivation works very well to improve passivation on Si. The PDA of SiN_x at an appropriate temperature can promote hydrogenation, which is known to improve the chemical passivation of Si.[36,37] The activation of the hydrogenation from the SiN_x passivation layer relies not only on the sufficient H source but also on the encapsulation effect.[38] Therefore, an ALD Al_2O_3 layer may act not only as a hydrogen source but also as an H diffusion barrier,[18,39] showing its high importance in the stack passivation structure. This could explain the efficient passivation obtained in the $Si/SiN_x/Al_2O_3$ samples.

An interesting difference between the passivation of Si and Ge surfaces with annealed SiN_x/Al_2O_3 stack is how the annealing affects the passivation efficiency and the properties of the substrate-thin film interface. In Ge, H can passivate some of the recombination-active interface defects, which is seen as an improved lifetime and a reduced D_{it} in annealed SiN_x/Al_2O_3 samples. However, H passivation is much less efficient in Ge

© 2022 The Authors. physica status solidi (a) applications and materials science published by Wiley-VCH GmbH

compared to Si,[40] which explains why efficient passivation cannot be achieved as in Si.

5. Conclusions

In this article, a surprisingly high negative Q_{tot} was found in PECVD SiN_x-passivated Ge samples, which was opposite to the Si substrate counterpart that had a high positive charge. This might be due to the abundant Ge surface trap states and SiN_x chargeable defect centers. The SRV_{max} of the SiN_x-passivated samples was reduced by a factor of three after a 400 °C PDA in FG ambient on both Si and Ge without affecting Q_{tot}. It was discovered that the deposition of an ALD Al_2O_3 capping layer followed by the PDA has a significant impact on further improving the surface passivation. For Si samples, an SRV_{max} as low as $2\,cm\,s^{-1}$ was achieved with a high positive Q_{tot} of $\sim 2.7 \times 10^{12}\,cm^{-2}$ and a low midgap D_{it} of $\sim 7 \times 10^{10}\,cm^{-2}\,eV^{-1}$. This low SRV_{max} could be explained by the combination of excellent field-effect passivation and chemical passivation. Also in the case of Ge, the Al_2O_3 capping layer reduced the midgap D_{it} to $\sim 4 \times 10^{11}\,cm^{-2}\,eV^{-1}$, resulting in an SRV_{max} of $17.5\,cm\,s^{-1}$. Interestingly, the negative Q_{tot} was simultaneously drastically reduced to a virtually neutral level with only $\sim -1.6 \times 10^{11}\,cm^{-2}$, which is a very different behavior compared to the Si counterpart. These results demonstrate a promising SiN_x-based passivation scheme for Ge-based devices, where low D_{it} and charge are favored.

Acknowledgements

The work was partially funded through the ATTRACT project funded by the European Union's Horizon 2020 research and innovation programme under grant agreement no. 101004462, by Business Finland (Project No. RaPtor 687/31/2019), by the Academy of Finland (Project Nos. 328482 and 331313), and by Tandem Industry Academia funding from the Finnish Research Impact Foundation. The work is also related to the Flagship on Photonics Research and Innovation "PREIN" funded by the Academy of Finland. The authors acknowledge the provision of facilities and technical support by the Micronova Nanofabrication Centre in Espoo, Finland, within the OtaNano research infrastructure at Aalto University.

Conflict of Interest

The authors declare no conflict of interest.

Data Availability Statement

The data that support the findings of this study are available from the corresponding author upon reasonable request.

Keywords

aluminum oxide, charge, germanium, interface defect density, silicon nitride, surface passivation

Received: October 5, 2022
Revised: November 9, 2022
Published online: December 20, 2022

[1] R. M. Wallace, P. C. McIntyre, J. Kim, Y. Nishi, *MRS Bull.* **2009**, *34*, 493.
[2] D. Kuzum, Jin-Hong Park, T. Krishnamohan, H.-S. P. Wong, K. C. Saraswat, *IEEE Trans. Electron Devices* **2011**, *58*, 1015.
[3] Y. Fukuda, Y. Yazaki, Y. Otani, T. Sato, H. Toyota, T. Ono, *IEEE Trans. Electron Devices* **2010**, *57*, 282.
[4] F. Bellenger, M. Houssa, A. Delabie, V. Afanasiev, T. Conard, M. Caymax, M. Meuris, K. De Meyer, M. M. Heyns, *J. Electrochem. Soc.* **2008**, *155*, G33.
[5] D. Kuzum, A. J. Pethe, T. Krishnamohan, Y. Oshima, Y. Sun, J. P. McVittie, P. A. Pianetta, P. C. McIntyre, K. C. Saraswat, in *2007 IEEE Inter. Electron Devices Meeting*, IEEE, Washington, DC **2007**.
[6] J. Isometsä, T. H. Fung, T. P. Pasanen, H. Liu, M. Yli-koski, V. Vähänissi, H. Savin, *APL Mater.* **2021**, *9*, 111113.
[7] W. J. H. Berghuis, J. Melskens, B. Macco, R. J. Theeuwes, L. E. Black, M. A. Verheijen, W. M. M. E. Kessels, *J. Appl. Phys.* **2021**, *130*, 135303.
[8] S. Dauwe, J. Schmidt, A. Metz, R. Hezel, in *Conf. Record of the Twenty-Ninth IEEE Photovoltaic Specialists Conf., 2002.*, IEEE, New Orleans, LA **2002**, https://doi.org/10.1109/PVSC.2002.1190481.
[9] B. Karunagaran, S. J. Chung, S. Velumani, E.-K. Suh, *Mater. Chem. Phys.* **2007**, *106*, 130.
[10] W. J. H. Berghuis, M. Helmes, J. Melskens, R. J. Theeuwes, W. M. M. E. Kessels, B. Macco, *J. Appl. Phys.* **2022**, *131*, 195301.
[11] H. Liu, in *presented at GADEST-19*, Mondsee, Austria, September **2022**.
[12] A. A. Dameron, S. D. Davidson, B. B. Burton, P. F. Carcia, R. S. Mclean, S. M. George, *J. Phys. Chem. C* **2008**, *112*, 4573.
[13] G. Dingemans, M. C. M. van de Sanden, W. M. M. Kessels, *Phys. Status Solidi RRL* **2011**, *5*, 22.
[14] B. Vermang, P. Choulat, H. Goverde, J. Horzel, J. John, R. Mertens, J. Poortmans, *Energy Procedia* **2012**, *27*, 325.
[15] K. Chen, W. Nemeth, S. Theingi, M. Page, P. Stradins, S. Agarwal, D. L. Young, in *2021 IEEE 48th Photovoltaic Specialists Conf. (PVSC)*, IEEE, Fort Lauderdale, FL **2021**.
[16] C. H. Poon, L. S. Tan, B. J. Cho, A. Y. Du, *J. Electrochem. Soc.* **2005**, *152*, G895.
[17] A. Satta, E. Simoen, R. Duffy, T. Janssens, T. Clarysse, A. Benedetti, M. Meuris, W. Vandervorst, *Appl. Phys. Lett.* **2006**, *88*, 162118.
[18] L. Helmich, D. C. Walter, D. Bredemeier, J. Schmidt, *Phys. Status Solidi RRL* **2020**, *14*, 2000367.
[19] M. Schofthaler, R. Brendel, G. Langguth, J. H. Werner, in *Proc. of 1994 IEEE 1st World Conf. on Photovoltaic Energy Conversion - WCPEC (A Joint Conf. of PVSC, PVSEC and PSEC)*, IEEE, Waikoloa, HI **1994**.
[20] S. W. Glunz, D. Biro, S. Rein, W. Warta, *J. Appl. Phys.* **1999**, *86*, 683.
[21] T. Lauinger, J. Schmidt, A. G. Aberle, R. Hezel, *Appl. Phys. Lett.* **1996**, *68*, 1232.
[22] G. Dingemans, W. M. M. Kessels, *J. Vac. Sci. Technol., A* **2012**, *30*, 040802.
[23] J. Schmidt, F. Werner, B. Veith, D. Zielke, S. Steingrube, P. P. Altermatt, S. Gatz, T. Dullweber, R. Brendel, *Energy Procedia* **2012**, *15*, 30.
[24] R. Hezel, R. Schörner, *J. Appl. Phys.* **1981**, *52*, 3076.
[25] G. Dingemans, N. M. Terlinden, M. A. Verheijen, M. C. M. van de Sanden, W. M. M. Kessels, *J. Appl. Phys.* **2011**, *110*, 093715.
[26] P. Repo, H. Savin, *Energy Procedia* **2016**, *92*, 381.
[27] M. A. Juntunen, J. Heinonen, V. Vähänissi, P. Repo, D. Valluru, H. Savin, *Nat. Photonics* **2016**, *10*, 777.
[28] G. Lucovsky, *J. Vac. Sci. Technol., B* **1996**, *14*, 2832.
[29] H. Mäckel, R. Lüdemann, *J. Appl. Phys.* **2002**, *92*, 2602.
[30] J. Robertson, *Philos. Mag. B* **1994**, *69*, 307.
[31] T. J. Grassman, S. R. Bishop, A. C. Kummel, *Surf. Sci.* **2008**, *602*, 2373.
[32] J. S. Lee, S. R. Bishop, T. J. Grassman, A. C. Kummel, *Surf. Sci.* **2010**, *604*, 1239.

© 2022 The Authors. physica status solidi (a) applications and materials science published by Wiley-VCH GmbH

18626319, 2023, 2, Downloaded from https://onlinelibrary.wiley.com/doi/10.1002/pssa.202200690 by Aalto University, Wiley Online Library on [05/02/2023]. See the Terms and Conditions (https://onlinelibrary.wiley.com/terms-and-conditions) on Wiley Online Library for rules of use; OA articles are governed by the applicable Creative Commons License

[33] J. R. Weber, A. Janotti, C. G. Van de Walle, *Phys. Rev. B* **2013**, *87*, 035203.
[34] A. Dimoulas, P. Tsipas, A. Sotiropoulos, E. K. Evangelou, *Appl. Phys. Lett.* **2006**, *89*, 252110.
[35] T. Nishimura, K. Kita, A. Toriumi, *Appl. Phys. Lett.* **2007**, *91*, 123123.
[36] B. Hallam, D. Chen, M. Kim, B. Stefani, B. Hoex, M. Abbott, S. Wenham, *Phys. Status Solidi A* **2017**, *214*, 1700305.
[37] T. N. Truong, D. Yan, W. Chen, M. Tebyetekerwa, M. Young, M. Al-Jassim, A. Cuevas, D. Macdonald, H. T. Nguyen, *Sol. RRL* **2020**, *4*, 1900476.
[38] D. Benoit, J. Regolini, P. Morin, *Microelectron. Eng.* **2007**, *84*, 2169.
[39] G. Dingemans, F. Einsele, W. Beyer, M. C. M. van de Sanden, W. M. M. Kessels, *J. Appl. Phys.* **2012**, *111*, 093713.
[40] A. Stesmans, T. Nguyen Hoang, V. V. Afanas'ev, *J. Appl. Phys.* **2014**, *116*, 044501.

© 2022 The Authors. physica status solidi (a) applications and materials science published by Wiley-VCH GmbH

18626319, 2023, 2, Downloaded from https://onlinelibrary.wiley.com/doi/10.1002/pssa.202200690 by Aalto University, Wiley Online Library on [05/02/2023]. See the Terms and Conditions (https://onlinelibrary.wiley.com/terms-and-conditions) on Wiley Online Library for rules of use; OA articles are governed by the applicable Creative Commons License